# An Implementation of *d*-, *q*- axis Control Technique of Two-kW Single Phase Grid Connected Converter for Wind Turbines

Jirawut Benjanarasut and Bunlung Neammanee*

***Abstract*— *This paper presents a 2-kW single phase grid connected converter for wind turbine. The converter uses a current control technique in the dq synchronous reference frame. This control method transforms single phase to two phases by shifting input phase by a quarter periods and transforms the stationary frame to the dq rotating reference frame. By decoupling control, the DC-bus voltage can be directly controlled by the direct axis current. The steady state current components become DC instead of AC. Experiments with a 2-kW wind turbine generator show that a controller is able to regulate a DC-bus by control the direct axis current reference with the excellent disturbance rejection and zero steady state error, which are suitable for wind turbine operation. Moreover for the grid side, the line current has low total harmonic distortion (THD) and a reactive power can be controlled to get a unity power factor.*

***Keywords*— Single phase grid connected, wind turbine, decoupling control, MPPT.**

## 1. INTRODUCTION

Wind energy has long been recognized as one of the alternative options for electricity production and is gaining increasing importance throughout the world because it is pollution-free, affordable and sustainable. In general, power from a wind turbine highly depends on wind speed (i.e., power increases rapidly with wind speed). Therefore, locating wind generators in a place where wind speed is strong and reasonably constant is an important factor. In addition to such a constraint, operating a wind power plant requires efficient control techniques to extract power from the turbines as much as possible for any input wind speed. In general, a wind turbine is mechanically designed to produce its rated power at a certain wind speed which is referred as rated wind speed.

The output energy from the wind turbine can be integrated into the grid, for a large size wind turbine, the stator of the doubly fed induction generator (DFIG) can be directly connected to the gird and the rotor connected to the grid via a small size back-to-back converter (25 - 30 % of its rated). For the synchronous generator, its connected to the grid via the larger size of a back-to-back converter and filter inductors.

The small size of wind turbine (lower than 5 kW) is connceted to the grid via a full bridge converter with maximum peak power tracking and a single phase grid connected converter. There are many types of single phase grid connected converters, depending on their control techniques. The single phase grid connected converter normally uses a voltage source inverter (VSI) to generate the output current into the grid. Hysteresis current controllers [1] have the advantage of simplicity and robustness, but the converters switching frequency largely depends on the load parameters and consequently the load current harmonics ripple is not optimal. It can be improved by the variable hysteresis band current control technique [2], [3]. However, its current ripple is still not optimal. For the ramp comparison control using a PI controller has a classical of use, but has the disadvantages of a steady state phase error between reference current and the output current, and also requires accurate tuning to suit load parameters.

This paper develops the sustainable technology for a single phase grid connceted converter for small wind turbine. The control technique and experiment are tested with a 2-kW single phase grid connected converter coupled to a permanent magnet synchronous generator and a wind turbine simulator system. The developed converter uses current control in the *d*-, *q*-axis (synchronous reference frame) of three phase converter to single phase converter. The main advantages of control in *d*-, *q*-axis makes the control variables look like DC quantities. Therefore it is easy to design an efficient controller. Moreover, the purposed converter can operate with low frequency response of current transducer, compared with hysteresis control because the converter uses the grid current for axis transformation.

This paper proposes a mathematical model development of a 2 kW single phase grid connected converter. The results obtained in Section 2 are used to build control block diagrams of the single phase grid connected converter that is presented in Section 3. The maximum peak power tracking (MPPT) control for wind turbine is explained in Section 4 and case studies are provided in Section 5. Section 6 concludes the paper.

## 2. MATHEMATICAL MODEL

To implement the purpose converter, its required a minimum of two independent phases in the system (*d*-, *q*-axis). It is necessary to create a second quantity in quadrature with the real one. Such a delay concept

Jirawut Benjanarasut and Bunlung Neammanee (corresponding author) are with Department of Electrical Engineering, Faculty of Engineering, King Mongkut's University of Technology North Bangkok, 1518 Pibulsongkram Road, Bangsue, Bangkok 10800. Phone: +66-81-841-9399; Fax: +66-2-585-7350; E-mail: amrx78@hotmail.com and bln@kmutnb.ac.th.

presented in this paper is shown in Fig.1. The real signal, $x(t) = x_\alpha(t)$, was delayed by 90 of the line period to form the virtual signal, $x_\beta(t)$, which is transformed to $x_d$ and $x_q$ in $d$-,$q$-axis by park transform.

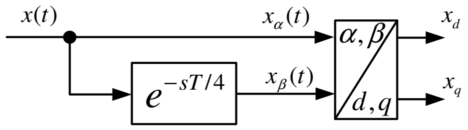


**Fig. 1. Transformation from to and in , axis.**

The schematic diagram of a power circuit of a single phase grid connected converter is shown in Fig.2, which is composed of a DC-bus capacitor, *C,* full bridge power switches, grid filter inductor, *L*, grid filter inductor parasitic resistance, *R* and the grid. The voltage equation of $v_{con}$ is shown in (1).

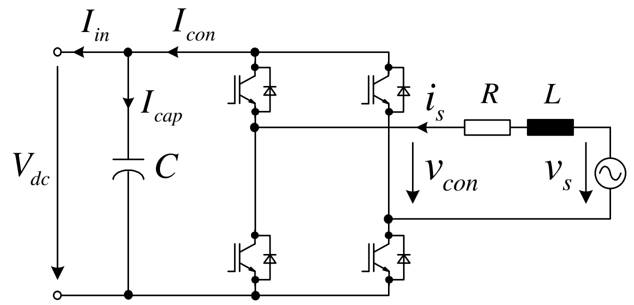


**Fig.2. Power circuit of a grid connected converter.**

$$v_s = Ri_s + L\frac{di_s}{dt} + v_{con} \tag{1}$$

Given $\Delta v = v_s - v_{con}$

$$L\frac{di_s}{dt} = \Delta v - Ri_s \tag{2}$$

$$L\frac{di_\alpha}{dt} = \Delta v_\alpha - Ri_\alpha \quad \text{and} \qquad L\frac{di_\beta}{dt} = \Delta v_\beta - Ri_\beta \tag{3}$$

Transform Eq. (3) in $d-,q-$axis, then

$$\Delta v_d = \Delta v_\alpha \cos\omega t + \Delta v_\beta \sin\omega t \text{ and} \qquad \Delta v_q = -\Delta v_\alpha \sin\omega t + \Delta v_\beta \cos\omega t \tag{4}$$

Transform current $i_s$ in figure 2 to $d-,q-$axis

$$i_{sd} = i_\alpha \cos\omega t + i_\beta \sin\omega t \text{ and} \qquad i_{sq} = -i_\alpha \sin\omega t + i_\beta \cos\omega t \tag{5}$$

Take derivative of Eq. (5) and multiply it by $L$

$$L\frac{di_{sd}}{dt} = -L\omega i_\alpha \sin\omega t + L\frac{di_\alpha}{dt}\cos\omega t + L\omega i_\beta \cos\omega t + L\frac{di_\beta}{dt}\sin\omega t \tag{6}$$

$$L\frac{di_{sd}}{dt} = -L\omega i_\alpha \sin\omega t + L\frac{di_\alpha}{dt}\cos\omega t + L\omega i_\beta \cos\omega t + L\frac{di_\beta}{dt}\sin\omega t \tag{7}$$

Substituting Eqs. (3) and (4) into Eqs. (8) and (9) respectively gives

$$\Delta v_d = L\frac{di_\alpha}{dt}\cos\omega t + Ri_\alpha \cos\omega t + L\frac{di_\beta}{dt}\sin\omega t + Ri_\beta \sin\omega t \tag{8}$$

$$\Delta v_q = -L\frac{di_\alpha}{dt}\sin\omega t - Ri_\alpha \sin\omega t + L\frac{di_\beta}{dt}\cos\omega t + Ri_\beta \cos\omega t \tag{9}$$

Rearrange Eqs. (8) - (9)

$$\Delta v_d = L\frac{di_{s\alpha}}{dt}\cos\omega t + L\frac{di_{s\beta}}{dt}\sin\omega t + Ri_{sd} \tag{10}$$

$$\Delta v_q = -L\frac{di_{s\alpha}}{dt}\sin\omega t + L\frac{di_{s\beta}}{dt}\cos\omega t + Ri_{sq} \tag{11}$$

Substitute Eqs.(10) - (11) in Eqs. (6) - (7) then

$$L\frac{di_{sd}}{dt} = L\omega i_{sq} + \Delta v_d - Ri_{sd} \quad \text{and} \qquad L\frac{di_{sq}}{dt} = -L\omega i_{sd} + \Delta v_q - Ri_{sq} \tag{12}$$

Substitute $\Delta v_d = v_{sd} - v_{cond}$ and $\Delta v_q = v_{sq} - v_{conq}$ in Eq. (12)

$$v_{cond} = -L\frac{di_{sd}}{dt} - Ri_{sd} + L\omega i_{sq} + v_{sd} \quad \text{and} \qquad v_{conq} = -L\frac{di_{sq}}{dt} - Ri_{sq} - L\omega i_{sd} + v_{sq} \tag{13}$$

Given $v_\alpha = V_m \cos\omega t$ and $v_\beta = V_m \sin\omega t$ . Transform $v_\alpha$ and $v_\beta$ into the $d-,q-$axis reference

$$v_{sd} = V_m \text{ and } v_{sq} = 0 \tag{14}$$

Substitute Eq. (14) in Eq. (13)

$$v_{cond} = -L\frac{di_{sd}}{dt} - Ri_{sd} + L\omega i_{sq} + V_m \tag{15}$$

$$v_{conq} = -L\frac{di_{sq}}{dt} - Ri_{sq} - L\omega i_{sd} \tag{16}$$

Converter power, $P_{con}$ in the grid connected converter in the $d-,q-$axis reference is shown in Eq. (19)

$$P_{con} = \frac{i_{sd} v_{sd}}{2} \tag{17}$$

Current $I_{con}$ , $I_{cap}$ and voltage $V_{dc}$ can be obtained from Eqs. (20) - (22)

$$I_{con} = \frac{P_{con}}{V_{dc}} = \frac{i_{sd} V_{sd}}{2V_{dc}} \tag{18}$$

$$I_{cap} = I_{con} - I_{in} \tag{19}$$

$$V_{dc} = \frac{1}{C} \int I_{cap} dt \tag{20}$$

Take Laplace transform of Eqs.(15) - (16) and (18) - (20)

$$v_{cond} = -i_{sd}(Ls + R) + L\omega i_{sq} + V_m \tag{21}$$

$$v_{conq} = -i_{sq}(Ls + R) + L\omega i_{sd} \tag{22}$$

$$V_{dc} = \frac{1}{sC} I_{cap} \tag{23}$$

$$I_{con} = \frac{i_{sd} V_{sd}}{2V_{dc}} = \frac{i_{sd} V_m}{2V_{dc}} \text{ and } I_{cap} = I_{con} - I_{in} \tag{24}$$

We can build a block diagram of single phase grid connected converter from Eqs. (21)-(24), which is shown in the box on the right hand side of Fig.3. It is clearly seen from the block diagram that the voltage $\omega Li_{sq}$ and $\omega Li_{sd}$ have a cross coupling term between $v_d$ and $v_q$. As a result, the DC-bus voltage depends on both parameters. To have independent control of the DC-bus voltage, the currents $i_{sq}$ and $i_{sd}$ are multiplied with $\omega L$ to compensate the coupling voltage as shown in the box on the left hand side of Fig.3. The voltage loop controls the DC-bus voltage using the voltage error as the input of a PI controller to generate the current reference $i_{sd}^*$, which can directly control the DC-bus voltage. The current reference $i_{sq}^*$ can independently control the reactive power [10] in the simulation by letting $i_{sq}^* = 0$ in order to obtain the unity power factor.

## 3. CONTROL BLOCK DIAGRAM OF SINGLE PHASE GRID CONNECTED CONVERTER

The overall control block diagram of grid connected converter shown in the right hand side of Fig.5 has two main parts. The first part is a power unit consisting of inductors, a power converter, DC-bus capacitors. The second part is a control unit in the lower part of the figure. The controller receives many parameters from the sensor such as grid voltage, line current, DC-bus voltage and load current. These parameters are necessary for Eqs. (21)-(24) for phase locked loop (PLL) [2-3]. The control variables are controlled in the synchronous reference frame by the PI controller.The control output transforms the stationary reference frame and construct the sinusoidal pulse width modulation (SPWM) signal to control the IGBTs in the power circuit. All of the control procedure is calculated based on the control block diagram and programmed by C language. The controller software is programmed on a Digital Signal Controller (DSC) for regulating the DC-bus voltage. The digital signal controller controls the system with two references. One is $i_{sq}^*$ for reactive power control (zero reactive power) and the other is $V_{dc}^*$ for DC-bus voltage control (400V). Both references are the inputs of PI controllers. The output of the controller will be changed to *d*-, *q*-axis voltage which is then transformed to three phase voltage. This voltage is converted to drive signal by the SPWM to control the converter.

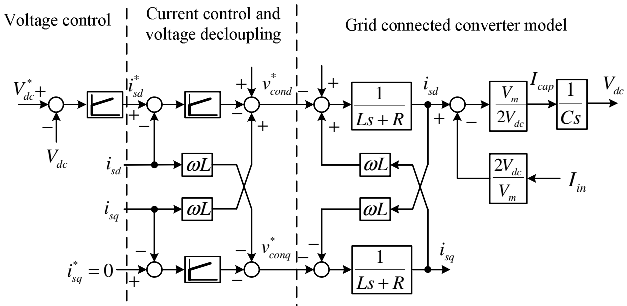


**Fig. 3. Block diagram of PI controller with voltage decoupling control.**

## 4. MAXIMUM PEAK POWER TRACKING FOR WIND TURBINE

The power captured by the wind turbine, $P_{turb}$ , is described in Eq.(5). The output power is a function of wind speed cube and power coefficient which depend on the wind characteristic and its operating point.

$$P_{turb} = \frac{1}{2} \rho \pi R^2 v_t^3 c_p(\lambda, \beta) \tag{25}$$

The tip speed ratio is mathematically expressed by

$$\lambda = \frac{\omega_t r}{v_t} \tag{26}$$

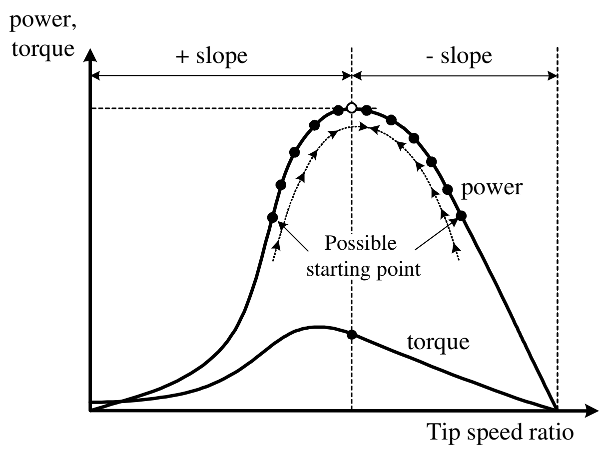


**Fig. 4. MPPT process.**

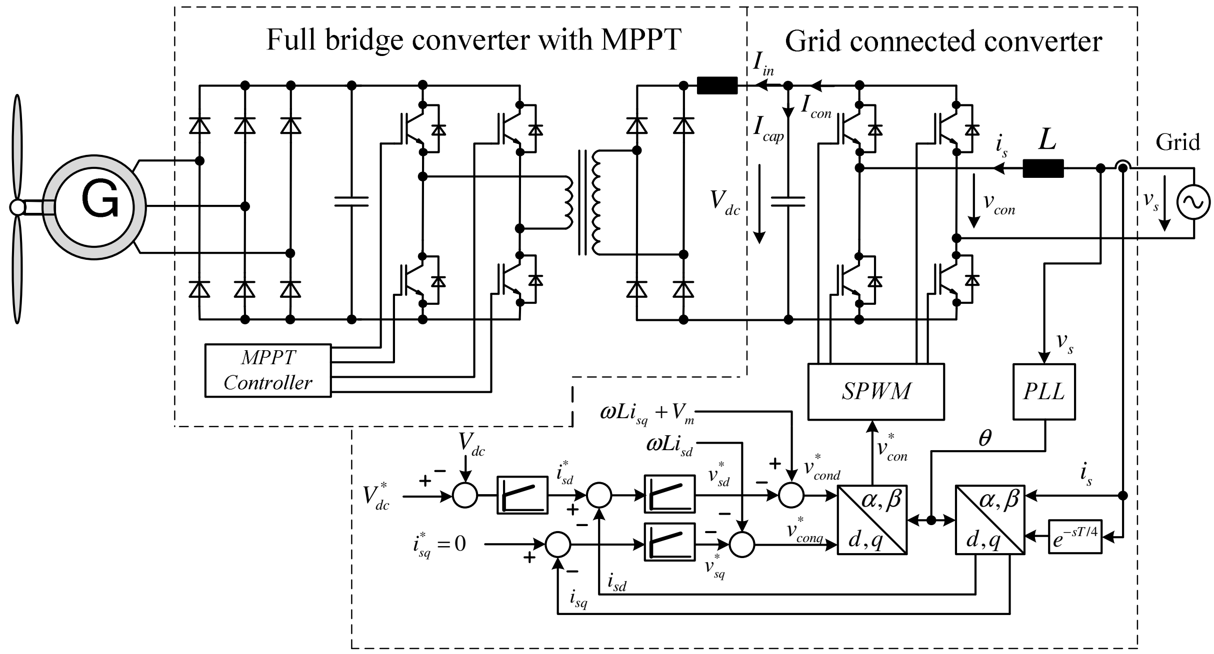


**Fig. 5. System control block diagram.**

The MPPT control algorithm is applied to maximize the wind turbine output power. Figure 4 shows typical characteristics of power and torque versus tip speed ratio of a wind turbine that needs to be controlled. The main purpose of the MPPT controller is to maintain the operating point at $P_m^{\max}$ for any wind speeds in the below rated wind speed region. At any instant of time, the operating point can be at the positive slope of the curve Fig.5 (the left hand side of the $P_m^{\max}$ occurs), or at negative slope (the right hand side of the $P_m^{\max}$). If an operating point is in the positive slope region, the controller will move it to the right hand side to get closer to the maximum. This can be achieved by decreasing load current, which results in an increase in rotational speed. Conversely, if the operating point lies on the right hand side of the peak, the load current has to be increased, resulting in a decrease in the rotational speed [11].

## 5. CASE STUDY

The test system is shown in Fig.6 composed of four main parts 1) DC supply for grid connected converter (used in the test mode) on the upper left hand side of the figure 2) a 5.5 kW wind turbine simulator source on the lower left hand side of the figure, 3) a purposed 2-kW single phase grid connected converter and full bridge converter with MPPT controller are in the upper right hand side, and 4) the control and the monitoring system in the lower of figure. The purposed 2-kW grid connected converter is composed of an inductor, discrete IGBTs for power circuit, IGBTs gate drive, a DC-bus capacitors, a bridge rectifier, transducers and a DSC-based control unit. The input of the converter is connected to full bridge with MPPT controller and the AC/DC source form wind turbine or other renewable. This system is designed to regulate the DC-bus voltage at 400 V. The normal grid voltage is 220V and grid frequency 50Hz. The design criterion and the system parameters are shown in table 1. The controller board of both converters uses a high performance 16 bits dsPIC30f6010 combining the advantage of a high performance 16-bit microcontroller (MCU) and a high computation speed digital signal processors. Software was implemented in this DSC and performed to link a personal computer via two RS232 ports. The picture of the real wind turbine simulator, a purposed 2-kW single phase grid connected converter and full bridge with MPPT controller is shown in Fig.7.

### *5.1 Performance of the 2-kW Grid Connected Converter*

The test system is shown in Fig.6. The experiment began by operating the converter to regulate the DC-bus voltage at 400 Vdc. Switch SW1 at postion 1 and SW2 is closed to step up a 2 kW DC power to DC-bus. When the system reached steady state condition, opened switch SW2. The output responses are shown in Fig.8.

In Fig.8, when SW2 was closed at $t_1$, the controller tried to regulate the DC-bus voltage at 400V. It is seen that stepping DC power caused an increase in the DC-bus voltage. The PI controller sent commands to increase current $i_{sd}$ to regulate the DC-bus voltage. It takes 400 milliseconds to reach steady state with an overshoot voltage of 7.5%. The line current, $i_s$, is increased to 8.4 $A_{rms}$ with 230 $V_{ac}$ and the output power direct connected to the grid. When switch SW2 is opened at $t_3$, the controller tried to regulate the DC-bus voltage at 400V. It can be seen that removing the DC power caused a decrease in the DC-bus voltage. The PI controller sent commands to decrease current $i_{sd}$ to regulate the DC-bus voltage. It takes 500 miliseconds to reach steady state with an overshoot voltage of 10%. The line current, $i_s$, is reduced to zero.

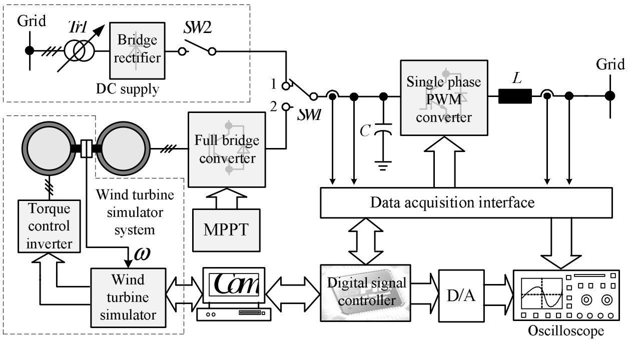


**Fig.6. Test system.**

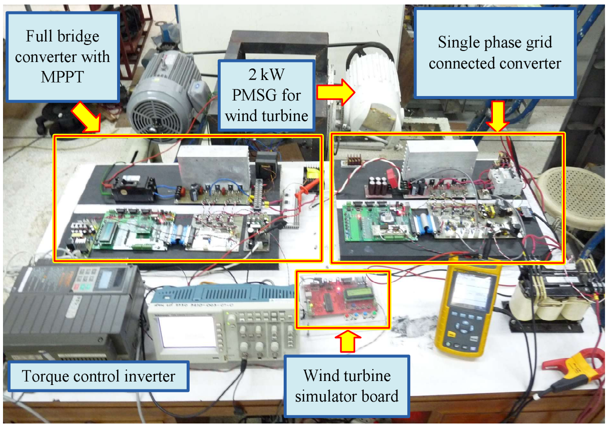


**Fig.7. 2 kW Single phase grid connected converter test system with 5.5 kW wind turbine simulator.**

**Table 1. Design criterion and system test parameters.**

| Parameters | Value |
|---|---|
| Electrical system | 1$\phi$, 2 wires, 50 Hz |
| Norminal voltage (rms) | 220 V |
| DC-bus voltage | 400 V |
| Rated power | 2 kW |
| $THD_i$ | IEEE 519-1992 |
| Power factor | -1.00 |
| DC-bus capacitor ( ) | 720 $\mu F$ |
| Grid filter inductor ( ) | 6 mH |
| Grid filter inductor parasitic resistance ($R$) | 0.4 Ω |
| Wind turbine generator type | 3$\phi$, PM synchronous |
| Generator voltage range | 150-650 $V_{L-L}$ |
| Full bridge converter rated power | 2.5 kW |
| Full bridge converter input voltage range | 200-650 $V_{DC}$ |

Figure 9 shows an extension period of Fig.8 during the grid connected converter supply 2 kW to the grid at steady state condition. Figure 9 a) show the line current and the grid voltage, the grid voltage $v_s$ is constant, the line current $i_s$ is 8.4 $A_{rms}$ near sinusoidal and the power factor factor is unity. Figure 9 b) show the current spectrum of the line current and the total harmonic distortion of the line current is 2.7 % with agree to the standard.

The THDi, power factor; PF, and efficiency of the purpose 2-kW single phase grid connected converter are shown in the table 2 during supply 25, 50, 75 and 100% of power rated to the grid. From the table, the $THD_i$ is inverse proportional to the output power and less than 5% when the output power more equal 1000 W. The power factor is near unity (PF ≅ -1.00) and the efficiency of the system between 94.5 to 95.5 %.

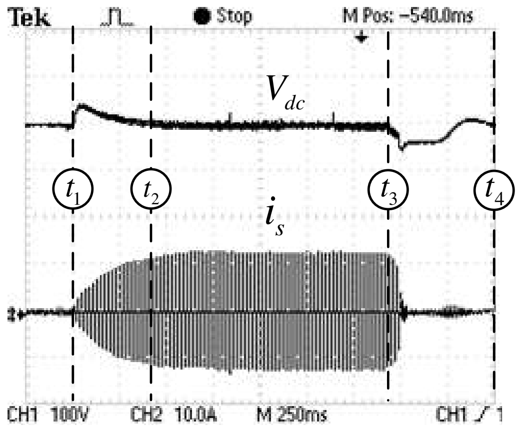


**Fig. 8. DC-bus voltage; $V_{dc}$ and the line current $i_{sd}$, $i_{sq}$, $i_s$ .**

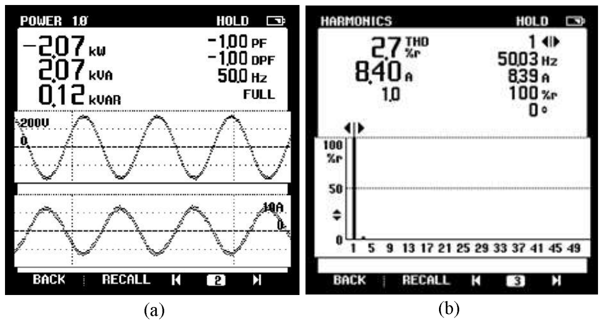


**Fig.9. a) line current, $i_s$ and grid voltage, $v_s$**
**b) percentage of total harmonic distortion of current ($THD_i$).**

**Table 2. THDi, PF and efficiency at Steady Stage**

| Power(W) | $THD_i$ (%) | PF | Efficiency (%) |
|---|---|---|---|
| 500 | 5.3 | -0.99 | 94.5 |
| 1000 | 4.6 | -1.00 | 94.8 |
| 1500 | 3.6 | -1.00 | 94.9 |
| 2000 | 2.7 | -1.00 | 95.5 |

### *5.2 MPPT of the Purpose System*

The MPPT control procedures was designed according to Fig.5 and programmed to the controller board of full bridge converter. The MPPT controller with the grid connected converter is tested with two conditions 1) step wind speed to verify the dynamic performance of the system and 2) variable wind speed to verify the tracking performance. To confirm the MPPT able to capture the maximum power, it is important to known the wind turbine characteristic of the test system. If the MPPT control can capture the maximum power, the operating point should stay on the top of each wind speed.

### *2 kW Wind Turbine Characteristics*

The wind turbine characteristic is tested by coulping the 5.5 kW wind turbine simulator with the 2-kW PMSG for wind turbine. The test procedures start by 1) generate a wind speed at 3 m/s, vary load and record the output power and rotational speed and 2) repeat step 1 but with wind speeds of 3.5, 4, ..., 7.5 m/s respectively. The ten output power versus rotational speed curves of 2-kW PMSG for wind turbine is shown in Fig.10.

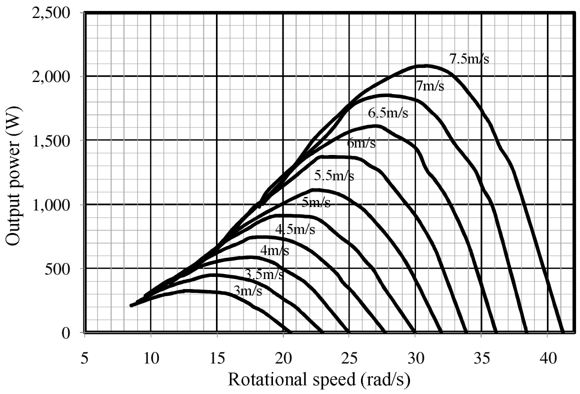


**Fig. 10. 2 kW PMSG for wind turbine characteristics with various wind speeds.**

### *Step Wind Speed*

For the test system in Fig.6, set the switch SW1 at position 2 and set the step reference wind speeds of 3.5, 6, 7.5, 6, 3.5 m/s to the wind turbine simulator. Run the test system and record the output power and the rotational speed. Figure 11 shows the step reference wind speeds with the corresponding generator output power. From the figure, it is clearly seen that the output power can track the reference wind speed in a short period of time and attempt to regulate the output power when the wind speed is constant.

To verify the MPPT controller able to capture the maximum power, it is important to plot the control trajectory of the output power with the wind turbine characteristics. Figure 12 shows the wind turbine characteristics (bold line) of Fig.10 and the control trajectory (plus sign) of Fig.11. From the figures, the control trajectory has a fast tracking to the maximum peak power for the step up/down wind speed and maintains at the maximum power (at each wind speed) when the wind speed is constant.

### *Variable Wind Speed*

With the same test system, set the random reference wind speeds as shown in Fig.13 a). The corresponding output power of wind turbine generator is shown in Fig.13 b). Form the figure, the output power can track the maximum power according to the random reference wind speed.

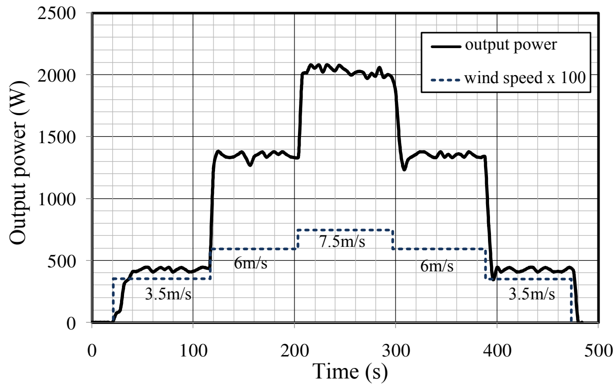


**Fig.11. The apply step wind speed (step up/down).**

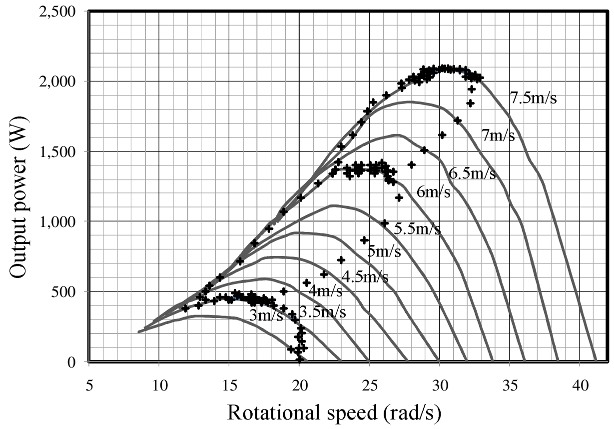


**Fig.12. The control trajectory of MPPT controller.**

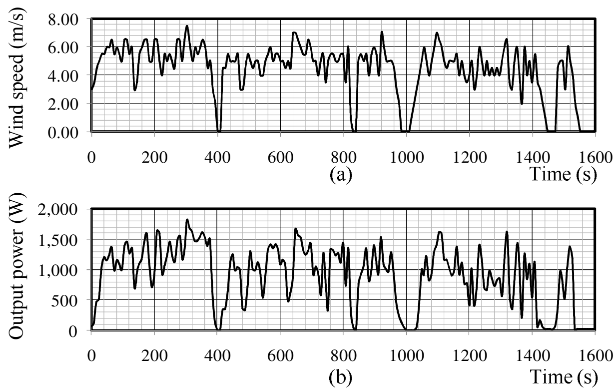


**Fig 13. a) variable wind speed and b) output power.**

## 6. CONCLUSION

A proposed *d*-, *q*- axis control technique of 2-kW single phase grid connected converter has the advantages of the decoupling control in the three phase system and improved control performance. This methodology transforms the control parameters in the stationary axis to the *d*-, *q*-axis by splitting single phase to two phases and uses the PLL for control. Additionally active and the reactive power are independently controlled by *d*-, *q*-axis current respectively.

The purposed control technique was verified by the experimental results of a case study. It is clearly seen from the results that the control system can regulate the

DC-bus with fast response to disturbance rejection, (increase or decrease the DC-bus voltage from the MPPT controller) low overshoot and high efficiency. Moreover, the total harmonic distortion of current on the grid side is low with power factor near unity.

## ACKNOWLEDGMENT

The authors would like to thank Department of alternative energy development and efficiency, Ministry of energy for financial support.

## NOMENCLATURE

| | | |
|---|---|---|
| $v_s$ | = | grid voltage |
| $i_s$ | = | line current |
| $v_{con}$ | = | grid connected converter output voltage |
| $v_{sd}, v_{sq}$ | = | *d*- and *q*-axis grid voltage |
| $i_{sd}, i_{sq}$ | = | *d*- and *q*-axis line current |
| $v_{cond}, v_{conq}$ | = | *d*- and *q*-axis grid connected converter output voltage |
| $V_m$ | = | peak grid voltage |
| $V_{dc}$ | = | DC-bus votage |
| $I_{con}$ | = | DC side converter current |
| $I_{cap}$ | = | DC-bus capacitor current |
| $I_{in}$ | = | DC side input current |
| | = | power captured by wind turbine |
| | = | air density |
| | = | turbine radius |
| $v_t$ | = | wind speed |
| $c_p$ | = | power coeffcient |
| $\beta$ | = | pitch angle |
| $\lambda$ | = | tip speed ratio |
| $\omega_t$ | = | turbine rotational speed |

## REFERENCES

[1] Plunkett, A.B. 1979. A current controlled PWM transistor inverted drive. In *Proc. IEEE IAS Annu. Meeting*. pp.: 785 – 792.

[2] Bose, B.K. 1990. An adaptive hysteresis–Band current control technique of a voltage-fed PWM inverter for machine drive system. In *IEEE Trans. Ind. Electron*., 37(5):402-408.

[3] Yao, Q. and Holmes, D.G. 1993. A simple novel method for variable Hysteresis- band current control of a three phase inverter with constant switching frequency. In *Proc. IEEE Ind. Appl. Meeting*, pp.: 1122-1129.

[4] Arman Roshan, Rolando Burgos, Andrew C. Baisden, Fred Wang and Dushan Boroyevich. 2007. A D-Q Frame Controller for a Full-Bridge Single Phase Inverter Used in Small Distributed Power Generation System. In *Applied Power Electronics Conference*, APEC 2007 - Twenty Second Annual IEEE, 25 Febuary-1 March, pp.: 641 – 647.

[5] Sudmee, W.and Neammanee, B. 2007. Control and Implementation of Line Side Converter for Doubly Fed Induction Generator of Wind Turbine. *Electrical Engineering, Electronics, Computer, Telecommunications and Information Technology (ECTI) International Conference*. Chiang Rai, Thailand, 9-12 May, pp.: 249-252.

[6] Krajangpan, K. Neammanee, B. and Sirisumrannukul, S. 2008. Control Performance of a MPPT controller with Grid Connected Wind Turbine. *The Greater Mekong Subregion Academic and Research Network (GMSARN) International Journal*, 2(1):7-14.

[7] Kaura, V. and Blasko, V. 1997. Operation of a Phase Locked Loop System Under Distorted Utility Condition. *IEEE on Industry Application*, 33(1):58-63.

[8] Yaosuo Xue, Liuchen Chang, Sren Baekhj Kjaer, Bordonau, J. Shimizu, T. 2004. Topologies of single-phase inverters for small distributed power generators: an overview. *IEEE Transactions on Power Electronics,* 19(5):1305-1314.

[9] B Singh, B.N. Singh, A. Chandra, K. Al-Haddad, A. Pandey, and D.P. Kothari. 2003. A review of single-phase improved power quality ac-dc converters. *IEEE Transactions on Industrial Electronics*; 50(5):962 –981.

[10] Andre Veltman, Duco W.J. Pulle, Rik W. De Doncker, L.G.B. Aredes, M. 2007. *Fundamentals of Electric Drives*. Spring-Verlag: Berlin Heidelberg.

[11] Neammanee, B. Krajangpan, K. Sirisumrannukul, S. and Chatratana, S. 2008. Maximum Peak Power Tracking-Based Control Algorithms with Stall Regulation for Optimal Wind Energy Capture. *The industry applications transaction, The Institute of Electrical Engineering of Japan (IEEJ)*;128(4):411-417.

[12] Neammanee, B. Sirisumranukul, S. Chatratana, S. 2007. Development of a Wind Turbine Simulator for Wind Generator Testing. *International Energy Journal (IEJ);*8(1): 21-28.